Effect of radio frequency power and total mass-flow rate on the properties of microcrystalline silicon films prepared by helium-diluted-silane glow discharge

I. Torres ⁎, R. Barrio, J.D. Santos, N. González, J.J. Gandía
Instituto de Energías renovables, CIEMAT, Avda. Complutense 22, E-28040 Madrid, Spain
E-mail address: ignacio.torres@ciemat.es

Abstract

Hydrogenated microcrystalline silicon thin films have been prepared by plasma-enhanced chemical vapor deposition at relatively low deposition temperatures (180 °C). Helium dilution of silane, instead of the more commonly approach of hydrogen dilution, has been used to promote microcrystalline growth. The effect of the applied radio frequency power (RFP) and the total gas flow on the structural, optical and electrical characteristics have been studied. As observed from the structural measurements, microcrystalline growth is favored as the applied RFP is increased and/or the total gas flow is decreased. Increasing the RFP however, brings associated an increase in the defect density in the amorphous tissue surrounding the crystalline grains and/or an increase in intra-grain defects as deduced from the structural, optical and electrical measurements. Microcrystalline growth and defect formation is rationalize in terms of the He* deexcitation process and high energy He+ ions bombardment.

Keywords: Microcrystalline silicon, Plasma-enhanced chemical vapor deposition, Optoelectronic properties, Structural properties, X-ray diffraction, Raman spectroscopy

1 Introduction

Hydrogenated microcrystalline silicon films (μc-Si:H) have seen a drastic increase in the interest shown by the scientific community over the last two decades [1–3]. Thin film technologies such as solar cells and thin film transistors [4] have been able to exploit the particular properties of microcrystalline silicon. Thin film transistors and solar cells are being developed based entirely in microcrystalline silicon [1,2,5] as well as in conjunction with amorphous [2] and crystalline silicon [6]. Due to the higher doping efficiency, higher carrier mobility and lower optical absorption compared to amorphous silicon films, doped microcrystalline silicon are currently being employed as window layers in amorphous silicon solar cells [7] and heterojunction solar cells [6]. In its undoped state, the improved infra- red response is exploited by using μc-Si:H films as absorber layer in the bottom cell of amorphous silicon/microcrystalline silicon tandem cells. This particular type of tandem cell is currently seeing such an impact that it has been individually named as micromorph cells [3,5,8,9].

There are several techniques that have been applied in the preparation of microcrystalline silicon such as plasma-enhanced chemical vapor deposition (PECVD), radio frequency sputtering, cyclotron resonance chemical vapor deposition or hot wire chemical vapor deposition (HW-CVD) among others. HW-CVD stands out for the large deposition rates that can be achieved; however, from the industrialization point of view, PECVD deposition of microcrystalline silicon is the most robust and easily scalable deposition method. To obtain the necessary conditions to deposit microcrystalline silicon films, one generally deposit the films from a mixture of H2 and SiH4. However, the gas dilution ratio alone does not determine whether a film will grow microcrystalline or not since also the silane depletion fraction has to be taken into account [10]. For this reason, microcrystalline films with similar properties can be deposited from, a priori, very different conditions (different flows, different applied radio frequency power (RFP), different pressures…). Even microcrystalline films can be grown from pure SiH4 under very high depletion conditions [11].

In addition to H2 dilution, microcrystalline films have been grown

using different inert gases such as Ar [12] or He [13–15] without adding any H2, probing that H2 dilution is not a necessity. What is attractive about inert gas dilution is the fact that high density plasmas can be obtained at low power, low pressure and low temperature. In addition, the TCO (transparent conductive oxides) substrates that can be used to deposit microcrystalline silicon from H2 dilution for solar cells application are limited to those that are not chemically reduced by hydrogen plasmas i.e. ZnO. By using an inert gas instead of H2, TCO's such as ITO or Sn2O could also be used without adding extra ZnO protective layers.

In the present work, microcrystalline films prepared from He dilution have been deposited and characterized structurally, optically and electrically. Through variations in the total gas flow (ϕT) and in the applied RFP a transition in the growing conditions from fully amorphous to films with up to 70% crystalline fraction can be observed. In the following, the experimental details will be presented and the effect of ϕT and the applied RFP during film preparation in the structural, optical and electrical characteristics will be discussed.

2 Experimental details

μc-Si:H films described in this work were deposited onto 10 × 10 cm2 soda lime glass substrates in a high-vacuum parallel- plate PECVD reactor using a 13.56 MHz excitation frequency. The reactor was equipped with a shower-head electrode of 272 cm2 situated at 2.2 cm from the grounded bottom electrode while

exhaust gases were pumped out of the system from one side of the chamber. The films were deposited from a mixture of SiH4 and He. Silane input concentration c(%) = 100 ×ϕSiH4 /(ϕSiH4 +ϕHe) was kept constant at 1% for all deposited films. Applied RFP was varied between 85 W and 195 W and ϕT between 175 sccm and 500 sccm. Both the pressure and the substrate temperature were kept at 93 Pa and 180 °C respectively throughout. Deposition time was varied so that all films had a thickness in the range 300 nm to 320 nm. No attempt has been made to reduce the oxygen content in the silane–helium mixture or to compensate via micro-doping the deposited films. Therefore, it is expected that the films deposited for this work present a slight n-type character as is typically observed [5].

The electrical, optical and structural characteristics of the films were studied as follows. Dark conductivity, σ_D, and photoconductivity were measured at room temperature in a coplanar configuration with evaporated aluminum contacts using a Keithley 617 electrometer. Illumination was provided with a class A solar simulator (Steuernagel SC575) at AM1.5G conditions and 100 mW/cm2. Film thickness and deposition rate were estimated from reflectance and transmittance spectra in the 250–2500 nm range obtained with a UV–vis–NIR spectrofotometer (Perkin Elmer, Lambda 950).

Micro-Raman spectroscopy (Renishaw Invia 1208-05 equipped with an Ar laser emitting at 514 nm) was also used to measure the so- called Raman crystallinity factor, Φ_C [16].

$$\Phi_C = I_{\mu(c)} / I_{\mu(c)} + I_a = (I_{520} + I_{510}) / (I_{520} + I_{510} + I_{480}),$$

where $I_{\mu(c)}$ and I_a represents the integrated Raman scattered intensities assigned to the crystalline and amorphous phase respectively. In practice, Φ_C can be evaluated from the ratio of the area of the deconvoluted peaks related to the crystalline fraction (due to both crystalline, I_{520}, and defective crystalline, I_{510}, phases) over the total area of the silicon-related peaks.

The Raman crystallinity factor underestimate the 'real' volume crystalline fraction and therefore should only be treated as a 'quick' laboratory check. In addition to Micro-Raman, X-Ray diffraction (XRD) patterns were acquired with an X'Pert-MPD (Philips) difractometer using CuK_α radiation (θ–2θ scans) to investigate the crystalline structure.

3 Results and discussion

The objective of this work was to study the joint effect of the applied RFP and the ϕ_T used when depositing microcrystalline silicon films from helium dilution. For this purpose, five different sets of samples were studied. Three of the five sets consist in films deposited using a ϕ_T of 350, 300 or 250 sccm while the applied RFP is swept between 85 W and 195 W. The other two sets consist in films deposited using a RFP of 100 W or 165 W while ϕ_T is swept between

500 and 175 sccm. In this section, the results obtained from the structural characterization (XRD and micro-Raman), optical characterization, and electrical characterization are presented.

3.1 Structural characterization

In order to study the changes in the different films structure due to variations in the applied RFP or ϕ_T, XRD patterns and micro-Raman spectra were monitored. In Fig. 1 an example of XRD patterns

obtained in four different films is plotted. As can be seen, either increasing the applied RFP or decreasing the ϕ_T used leads to a partial crystallization of the films. The same behavior with RFP and ϕ_T can be found in the literature for μc-Si:H films deposited from He or H_2 dilution [10,15,17-19]. The four films shown are part of only two of the different series but Fig. 1 displays perfectly what is observed for the five different series under study. The three peaks corresponding to the ⟨ 111⟩ , ⟨ 220⟩ and ⟨ 311⟩ crystallographic orientation of crystalline silicon are readily identified at $2\theta \approx 28.3°$, 47.3° and 56° respectively.

For the films deposited from a constant ϕT, the peaks in the XRD pattern appear only if the applied RFP value is above a minimum which depends on the ϕT value used. Above this RFP value, the grain sizes calculated from the ⟨111⟩ and ⟨220⟩ orientations following Scherrer's formulation remained constant at ~ 10 nm and ~ 6 nm irrespective of the ϕT value used. Similarly, microcrystalline grains in the XRD patterns of the films deposited at constant RFP are only detected if ϕT is below a certain value that depends on the RFP used. The calculated grain sizes at this ϕT value are also ~ 10 nm and ~ 6 nm for the ⟨111⟩ and ⟨220⟩ orientations and remain unchanged with further reduction in ϕT.

Micro-Raman measurements were used to determine the crystal- line fraction of the films as explained in the Experimental details section. Fig. 2 shows ΦC as a function of the applied RFP and ϕT for the different sets of films studied. As can be observed, for the films deposited from a constant ϕT the Raman crystalline fraction increases with increasing RFP and the maximum value achieved is higher at lower ϕT [17]. In addition, the RFP value at which the onset of microcrystal formation occurs decreases and the amorphous to microcrystalline transition becomes less abrupt with decreasing ϕT.

For the films deposited at constant RFP, an amorphous to microcrystalline silicon transition is also observed as the ϕ_T used is swept from high values towards moderate values [17]. As it occurs with the films deposited from a constant ϕ_T, the maximum Raman crystalline fraction achieved and the position of the transition shows a dependency with the RFP used. As its value decreases, the maximum Raman crystallinity and the ϕ_T value at which the transition occurs decreases.

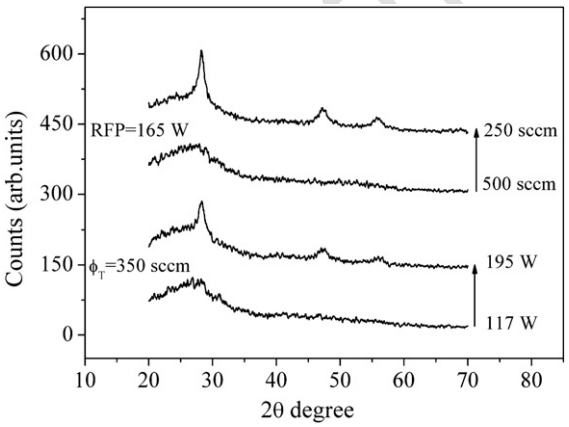

Fig 1: XRD patterns of four different films showing the film structural change when the applied RFP is increased (from 117 W to 195 W) or the total gas flow is decreased (from 500 sccm to 250 sccm).

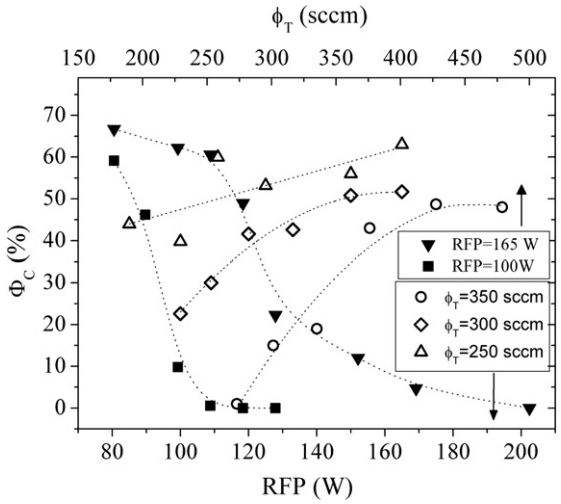

Fig. 2. Raman crystalline factor, Φ_C, vs applied RFP (bottom axis) and total gas flow,ϕ_T, (top axis) for the different films under study. Closed symbols refer to films deposited at a fixed RFP value (165 W and 100 W) while the total gas flow is varied. Open symbols refer to films deposited from a fixed total gas flow (350, 300 and 250 sccm) while the applied RFP value is varied. Open and closed symbols maintain the same correspondence in following figures. Lines are guides to the eye only.

3.2 Optical characterization

The optical properties of the different sets of films were also studied from the transmittance/reflectance spectra. The optical absorption coefficient measured at a particular energy of 2.5 eV, α(2.5 eV) [18], for the different sets of data discussed above is shown in Fig. 3 as a function of RFP and ϕT, as corresponding. As can be seen from the films deposited from a constant ϕT, using higher ϕT values leads to films having higher optical absorption while increasing the applied RFP lead to films with continuously decreasing optical absorption [15,18]. Similar to what was observed in the Raman spectra, the optical absorption presents a tendency to saturate as RFP is increased beyond certain value and this particular value decreases as ϕT decreases. As expected, the optical absorption of the films deposited with the RFP set to 100 W or 165 W also sees a gradual reduction as ϕT decreases.

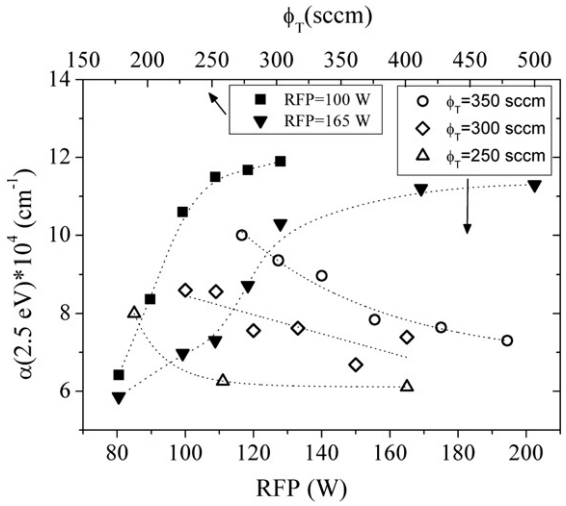

Fig. 3. Optical absorption coefficient measured at a particular energy of 2.5 eV, α(2.5 eV), vs applied RFP (bottom axis) and total gas flow, ϕ_T, (top axis) for the different films under study.

3.3 Electrical characterization

The electrical characteristics (σ_D and photosensitivity) of all the films under study were also measured. In Fig. 4, σ_D is plotted as a function of the applied RFP during film deposition for the three different total flows (350, 300 and 250 sccm). For all three set of data, σ_D increases with increasing RFP [18] until saturation is reached. Only in the case of ϕ_T = 300 sccm a slight decrease in σ_D is observed after reaching a maximum. As can be seen, for a given RFP value the films are more conductive as the ϕ_T used is decreased, concomitant with the increase in crystallinity observed in Fig. 2.

In Fig. 4, the variations in σ_D with ϕ_T can also be observed for the two sets of films deposited with an RFP of 100 W and 165 W. As can be seen, regardless of the applied RFP, σ_D increases as ϕ_T decreases. In addition, σ_D is always higher for the films deposited from the highest RFP value used. Again, this is in accord with the crystallinity data presented in Fig. 2

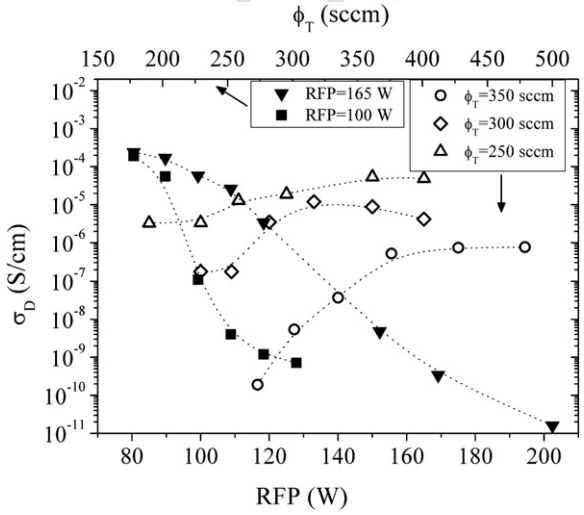

Fig. 4. Dark conductivity, σ_D, vs applied RFP (bottom axis) and total gas flow, ϕ_T, (top axis) for the different films under study.

3.4 Discussion

The results shown in Figs. 1 and 2 show that it is possible to obtain microcrystalline silicon from He dilution by either varying the applied RFP or the ϕ_T used to deposit the films within an appropriate range. The optical and electrical characteristics shown in Figs. 3 and 4 also evince a gradual transition from an amorphous dominated structure towards a moderate microcrystalline network. At high ϕ_T and low RFP, the optical absorption is high while the dark conductivity is low concomitant with the films being highly amorphous. By either decreasing ϕ_T or increasing RFP, both the optical absorption decreases and the dark conductivity increases as it is expected to happen as the film crystalline fraction increases up to moderate values. This can be more clearly seen in Figs. 5 and 6 where, α(2.5 eV), and σ_D, as a function of Φ_C, are shown. As the film Φ_C increases, it becomes less light absorbing while σ_D increases, showing a tendency to saturate at the highest values of Φ_C achieved. As can be observed, for a particular value of Φ_C a range of α(2.5 eV) values and σ_D values can be measured depending on the deposition parameters. Since we are comparing films with similar Φ_C and similar grain sizes the measured differences have to be related to the grains' crystalline structure or to the amorphous tissue in which the nano-crystals are embedded. To understand these differences, it is necessary to understand the effect of RFP and ϕ_T on the deposited films.

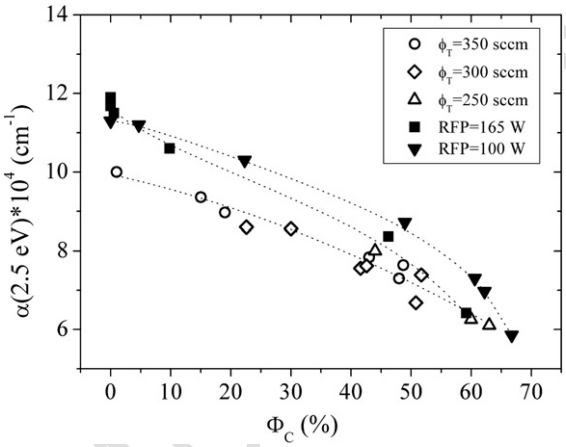

Fig. 5. Experimental relationship between the measured optical absorption coefficient, α(2.5 eV), and the calculated Raman crystalline factor, Φ_C, for the different films under study.

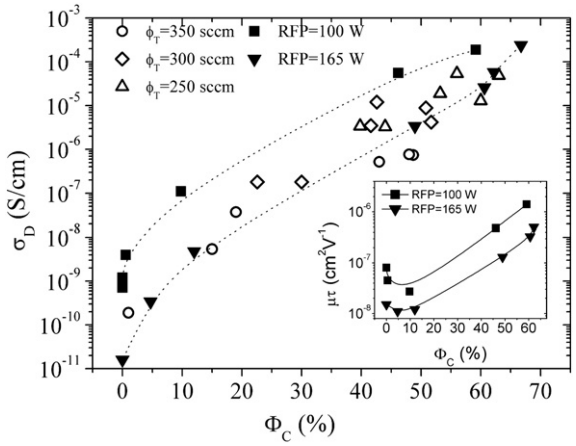

Fig. 6. Measured dark conductivity, σD, vs Raman crystalline factor, ΦC, for the different films under study. Inset shows the calculated μτ product vs ΦC for the sets of films deposited at a fixed RFP value (165 W and 100 W).

Let's consider first the effect of the applied RFP to explain the present results. Since the films are being deposited from a strictly 100% He dilution with no added H_2, it has to be taken into consideration the effect that ionized He^+ and metastable He* have on the plasma and on the growing surface. In He diluted SiH_4 plasmas, in addition to the regular process of electron impact dissociation of SiH_4 molecules, energy transfer from He metastable states plays an important role in SiH_4 dissociation [15]. Thereby, typically higher density plasmas and higher deposition rates are achieved at the same applied power when compared to H_2 diluted SiH_4 plasmas [14].

Metastable He* is believed to be responsible for the transition from a-Si:H growth to μc-Si:H growth [15]. When He* atoms reach the growing surface at thermal velocities, the deexcitation energy of He* to its ground state is absorbed by the lattice of the growing film. This energy is used for breaking strained weak Si-Si bonds at the boundary of c-Si nucleation centers and the amorphous matrix, allowing the formation of stronger bonds.

On the other hand, the sputtering caused by high energy He^+ ions impinging the surface can gradually lead to a more rough surface and void-rich films. Since the formation energy of He^+ (24 eV) is higher than that of He* (20 eV), their relative importance will depend on the RFP applied.

At low RFP values, the effect of He^+ ion bombardment is significantly lower than that of He* and hence microcrystalline growth is promoted as RFP is increased which is what is observed in the present results. But as the applied RFP is further increased, the He^+ ion density also increases and its effect on the growing surface would become more noticeable. As a result, higher defect densities within the films would be present.

Although hidden, this assertion can be deduced from the results shown in Fig. 5. Focusing in the two sets of films deposited with a fixed RFP value and varying ϕ_T (filled symbols) it is clear that for every value of Φ_C the measured optical absorption is systematically higher in the set of films deposited with RFP= 165 W (filled triangles) than in the set of films deposited with RFP= 100 W (filled squares). Since α(2.5 eV) continuously decreases with Φ_C, the fact that, for two films having a similar α(2.5 eV)

Φ_C is higher in the case of RFP= 165 W suggests that the films deposited at higher RFP are more defective.

In Fig. 6, a similar discrepancy in the measured dark conductivity can be observed between the films deposited with RFP= 100 W and RFP= 165 W for a similar value of Φ_C. In the range of Φ_C values where both sets of films can be compared, the films deposited with RFP= 100 W present a dark conductivity higher than the films deposited with RFP= 165 W. The inset included in Fig. 6 represent the mutau ($\mu\tau$) product of both series in the range of Φ_C values up to 60%. As can be seen, the $\mu\tau$ product of the films deposited with RFP= 100 W is also systematically higher than the films deposited with RFP= 165 W. Since from optical measurements it was concluded that a more defective film is obtained in the case of films deposited with higher RFP values this new representation suggests that the created defects are also electrically active and limit to some extent the electronic transport in the films.

Regarding the effect of the total gas flow used, the transition between a-Si:H and μc-Si:H is achieved by controlling the gas residence time in the plasma [19]. Since:

$$t_{dw} = \frac{pV}{\phi_T}$$

if ϕ_T decreases, t_{dw} increases and the probability that a silane molecule is decomposed and an He atom is ionized/excited through electron impact increases. Therefore, at a given RFP value, a decrease in ϕ_T leads to an increase of the energy transfer from the deexcitation of He* to the growth surface and hence, to an increase in microcrystallinity. Hence, while at high ϕ_T it is necessary to apply high RFP values to deposit microcrystalline films, at low values of ϕ_T microcrystalline films can be deposit even at moderate or low RFP values as shown in Fig. 2 (open symbols). Furthermore, from the results shown in Fig. 2, it is clear that films with Raman crystallinity in excess of 50% could only be achieved when ϕ_T was lower than 300 sccm. In addition to the decrease in gas residence times, deposition rates increase with increasing ϕ_T values because of a higher availability of growth precursors. In excess, this is known to have a detrimental effect in the quality of films deposited under certain conditions. If the film growth is too fast, then the mechanisms leading to microcrystalline growth [15,20], such as precursors having enough time to reach a most favorable site, may not take place. Under these conditions, the film may not be able to surpass a certain degree of crystallinity by simply increasing RFP, which is what is observed in Fig. 2.

In Fig. 5, the experimental σ(2.5 eV) vs Φ_C of the three sets of films deposited with a constant ϕ_T and varying RFP is also represented (open symbols). Contrary to what it is observed in the case of films deposited from a constant RFP and varying ϕ_T (closed symbols), the experimental data of the three sets is reduced to nearly a single curve (aside some scattering in the mid-crystallinity region). Hence, it is not possible to evaluate the relative difference in the number of defects between the three sets of films deposited from different values of ϕ_T as done previously. However, it leaves clear again that in order to obtain highly microcrystalline films it is necessary to use relative low gas flows and high RFP values.

The experimental σ_D vs Φ_C represented in Fig. 6 for these sets of data (open symbols) also exhibit some scattering similar to what is observed in the optical data shown in Fig. 5. However, examining the data in the range of mid Φ_C values shows that the films deposited at the highest ϕ_T values used (350 sccm) present

the lowest σ_D values. The films deposited from $\phi_T = 300$ and 250 sccm present similar σ_D values, although the maximum conductivity measured correspond with the highest values of Φ_C attained in the films deposited from $\phi_T = 250$ sccm. Similarly, for the three sets of films, the $\mu\tau$ product is lowest for the films deposited from the highest ϕ_T for a similar value of Φ_C (not shown). Therefore, even though the scattering in the optical and the electrical data hinders a clear relationship between these results and the defects in the films, it still suggests an increase in the defect density with increasing ϕ_T.

Therefore, it can be reasoned out that the effects of RFP and ϕ_T considered in the preceding paragraphs account for the observed results in Figs. 5 and 6. Given a Raman crystalline fraction, the absorption coefficient is higher for the films deposited at higher RFP and/or higher ϕ_T. The higher optical absorption and the lower dark conductivity together with the lower $\mu\tau$ product is likely to be related to the presence of a higher defect density due, in one case, to the bombardment of high energy ions, and in the other, to an increase in the deposition rate.

4 Conclusions

Hydrogenated silicon films deposited by RF-PECVD from a SiH_4 and He mixture, with no added H_2 have been studied. The effect of the deposition applied RFP and total gas flow has been studied through structural, optical and electrical measurements in a wide range of values. Microcrystallization of the films can be achieved by either increasing the applied RFP or by decreasing ϕ_T. By increasing the applied RFP, the increase in energy density transferred to the growing surface from the He* deexcitation process promotes crystallization. On the other hand, decreasing ϕ_T increases the gas residence time and hence the probability of electron impact dissociation of SiH_4 and excitation of He atoms to He*. In general, for films with similar crystalline volume fraction and similar crystallites grain sizes the dark conductivity and the $\mu\tau$ products are lower and the optical absorption is higher at higher values of RFP and/or higher values of ϕ_T. This indicates the presence of a higher density of defects in the amorphous tissue and/or intra-grain defects at those deposition conditions. Probably, the higher density of defects originates from high energy ions (He^+) impinging the growing surface in the case of high RFP values and to an increase in the deposition rate above a certain value in the case of an increase in ϕ_T.

Acknowledgements

This work has been partially supported by the European Commission, VI Framework Program, under project ATHLET (contract no. 19670). The authors would like to thank Dr. Fernando Perales for micro-Raman measurements.

References

[1] J. Meier, R. Fluckinger, H. Keppner, A. Shah, J. Appl. Phys. 65 (1994) 860.

[2] O. Vetterl, F. Finger, R. Carius, P. Hapke, L. Houben, O. Kluth, A. Lambertz, A. Mück, B. Rech, H. Wagner, Sol. Energy Mater. Sol. Cells 62 (2000) 97.

[3] F. Meillaud, A. Feltrin, D. Dominé, P. Buehlmann, M. Python, G. Bugnon, A. Billet, G. Parascandolo, J. Bailat, S. Fay, N. Wyrsch, C. Ballif, A. Shah, Philos. Mag. 89 (2009) 2599.

[4] M. Forondona, D. Soler, J. Escarré, J. Villar, J. Bertomeu, J. Andreu, A. Saboundji, N. Coulon, T. Mohammed-Brahim, Thin Solid Films 501 (2006) 303.
[5] J. Meier, S. Dubail, R. Flückiger, D. Fischer, H. Keppner, A. Shah, IEEE First World Conference on Photovoltaic Energy Conversion Proceedings, Hawaii, U.S.A., December 5-9, 1994, p. 409.
[6] M.W.M. van Cleef, J.K. Rath, F.A. Rubinelli, C.H.M. van der Werf, R.E.I. Schropp, W.F. van der Weg, J. Appl. Phys. 82 (1997) 6089.
[7] J.K. Rath, R.E.I. Schropp, Sol. Energy Mater. Sol. Cells 53 (1998) 189.
[8] J. Meier, S. Dubail, J. Cuperus, U. Kroll, R. Platz, P. Torres, J.A. Anna Selvan, P. Pernet, N. Beck, N. Pellaton Vaucher, Ch. Hof, D. Fischer, H. Keppner, A. Shah, J. Non-Cryst. Solids 227 (230) (1998) 1250.
[9] A. Shah, J. Meier, E. Vallat-Sauvain, C. Droz, U. Kroll, N. Wyrsch, J. Guillet, U. Graf, Thin Solid Films 403–404 (2002) 179.
[10] B. Strahm, A.A. Howling, L. Sansonnens, Ch. Hollenstein, Plasma Sources Sci. Technol. 16 (2007) 80.
[11] B. Strahm, A.A. Howling, L. Sansonnens, Ch. Hollenstein, U. Kroll, J. Meier, Ch. Ellert, L. Feitknecht, C. Ballif, Sol. Energy Mater. Sol. Cells 91 (2007) 495.
[12] U.K. Das, P. Chaudhuri, S.T. Kshirsagar, J. Appl. Phys. 80 (1996) 5389.
[13] J. Cárabe, J.J. Gandía, N. González, A. Rodríguez, M.T. Gutiérrez, Appl. Surf. Sci. 143 (1999) 11.
[14] O. Saadane, S. Lebib, A.V. Kharchenko, C. Longeaud, P. Roca i Cabarrocas, J. Appl. Phys. 93 (2003) 9371.
[15] K. Bhattacharya, D. Debajyoti, Nanotechnology 18 (2007) 415704.
[16] C. Droz, E. Vallat-Sauvain, J. Bailat, L. Feitknecht, J. Meier, A. Shah, Sol. Energy Mater. Sol. Cells 81 (2004) 61.
[17] A. Chowdhury, S. Mukhopadhyay, S. Ray, Sol. Energy Mater. Sol. Cells 92 (2008) 385.
[18] D. Das, M. Jana, A.K. Barua, J. Appl. Phys. 89 (2001) 3041.
[19] T. Roschek, B. Rech, J. Müller, R. Schmitz, H. Wagner, Thin Solid Films 451 (2004) 466.
[20] A. Matsuda, Thin Solid Films 337 (1999) 1.